JOURNAL OF COMPUTATIONAL PHYSICS **125,** 150–160 (1996)
ARTICLE NO. 0085

How to Prevent Pressure Oscillations in Multicomponent Flow Calculations: A Quasi Conservative Approach

RÉMI ABGRALL

INRIA, BP 93, 06 902 Sophia Antipolis Cedex, France

Received December 20, 1994; revised July 20, 1995

A new numerical scheme for computing multicomponent flows is presented. It is able to handle strong shocks, is pressure oscillation free through the contact discontinuities, and guarantees the positivity of mass fractions. Some numerical experiments on shock tubes indicate the convergence to the correct weak solution. Comparisons with classical finite volume schemes are also proposed.

In this paper, we are interested in the simulation of multicomponent nonreacting flows. The thermodynamical assumptions are:

• the gas is a mixture of *ns* calorically perfect gases Σ_i. Their equation of state is

$$\varepsilon_i = \rho_i c_{vi} T, \tag{1}$$

where ε_i is the internal energy of the species Σ_i, ρ_i is its density, T if the temperature, and the specific heat c_{vi} is independent of T,

• the pressure is given by Dalton's law.

Without loss of generality, we may assume that $ns = 2$.

This kind of problem has already been widely studied; see [8, 1, 6, 5], for example. The classical finite volume type of schemes are usually faced with two major difficulties: the mass fractions Y and $1 - Y$ may become negative; the pressure may present oscillations through contact discontinuities, instead of remaining continuous. These difficulties are intimately related to their "finite volume" nature.

Let us describe some remedies.

Positivity. A modification of the numerical flux introduced by Larrouturou [6] enables us to guarantee the positivity of mass fractions under a CFL-like condition. This modification does not prevent pressure oscillations [2].

Pressure. S. Karni has introduced a nonconservative scheme that enables us to properly simulate the contact discontinuities (see [4, 5]). The positivity of a mass fraction is also guaranteed. The conservation errors are controlled, but this scheme cannot handle strong shocks. The conservation errors become so large that the solution no longer converges to the right one. See Hou and Le Floch [3] for a study of this kind of problem.

1. PROBLEM DESCRIPTION

The internal energy of each species Σ_i follows (1) thus the total internal energy is

$$\varepsilon = \rho c_v T, \tag{2}$$

where $\rho = \rho^{(1)} + \rho^{(2)}$ and

$$c_v = Y^{(1)} c_{v1} + Y^{(2)} c_{v2}.$$

The relation between the pressure p and the internal energy is

$$p = (\gamma - 1)\varepsilon, \tag{3}$$

where

$$\gamma = \frac{Y^{(1)} c_{p1} + Y^{(2)} c_{p2}}{Y^{(1)} c_{v1} + Y^{(2)} c_{v2}}. \tag{4}$$

As usual, we have set $c_{p1} = \gamma_i c_{vi}$. We often denote $\gamma - 1$ by κ. The total energy per unit volume is

$$E = \varepsilon + \tfrac{1}{2}\rho u^2;$$

here u is the velocity.

Several equivalent sets of partial differential equation may be considered for this model. They are written as

$$\frac{\partial W}{\partial t} + \frac{\partial F(W)}{\partial x} = 0$$

and have the same weak solutions. We display some examples:

0021-9991/96 $18.00

1. Symmetric formulation ([1], for example)

$$W = \begin{pmatrix} \rho^{(1)} \\ \rho^{(2)} \\ \rho u \\ E \end{pmatrix}, \quad F(W) = \begin{pmatrix} \rho^{(1)} u \\ \rho^{(2)} u \\ \rho u^2 + p \\ u(E+p) \end{pmatrix}. \tag{5}$$

2. Unsymmetric formulation ([6, 5], for example)

$$W = \begin{pmatrix} \rho \\ \rho Y \\ \rho u \\ E \end{pmatrix}, \quad F(W) = \begin{pmatrix} \rho u \\ \rho Y u \\ \rho u^2 + p \\ u(E+p) \end{pmatrix}. \tag{6}$$

3. "Gamma" formulation ([8], for example)

$$W = \begin{pmatrix} \rho \\ \rho\gamma \\ \rho u \\ E \end{pmatrix}, \quad F(W) = \begin{pmatrix} \rho u \\ \rho\gamma u \\ \rho u^2 + p \\ u(E+p) \end{pmatrix}. \tag{7}$$

These three formulations are equivalent, since γ is an homographic function of the mass fractions.

The major drawback of the finite volume formulations that can be rewritten (in their first-order version) as

$$W^{n+1} = P \cdot E \cdot W^n,$$

is not the evolution operator E (since even when it is exact, the same problem on the pressure exists) but lies in the projection operator P. To illustrate this, let us consider the system (5) for a contact discontinuity, where the Mach number is large enough for the finite volume scheme to reduce to

$$W_i^{n+1} = W_i^n - \lambda[F(W_{i+1}^n) - F(W_i^n)];$$

thus all that follows is valid for any finite volume numerical scheme. We assume for the sake of simplicity that the pressure is uniform ($p_j^n = p$, for all j), as well as the velocity ($u_j^n = u$). As it is shown in [1] and systematically exploited in [2], the first iteration of the scheme preserves the velocity u but the value of p_i^{n+1} is different of p. In [5], the same kind of analysis is done for the Roe scheme adapted to various multicomponent models.

The explanation is the following. The evolution of partial densities, momentum, and energy are independent. The pressure is obtained through the energy by γ, the density, and the momentum. The value of γ is computed from those of $\rho^{(1)}$ and $\rho^{(2)}$. The four conserved quantities are the average of the exact values in the cells. Thus the value of γ is an "averaged" value that does not correspond the value that would have been needed to preserve the pressure. Once the pressure is wrong in one cell, the velocity will go wrong at the next time step, and so on. The situation is more or less serious, depending on the initial conditions. Quirk and Karni [7] give an example where the numerical solution has little to do with the exact one. It can be easily understood that in combustion or detonation problems, the presence of a stiff source term can amplify this deficiency.

In [5], this problem is solved by using a nonconservative formulation of the Euler equation with primitive variables. Karni notices that the evolution of p only depends, in this formulation, on the gradients of p and u. Since they vanish through a contact discontinuity, p should remain constant.

In what follows, we show how to modify a finite volume scheme in order to prevent pressure oscillations. We illustrate this technique when Roe's Riemann solver is employed. We show the first-order and second-order versions of this scheme. We show that it is robust enough to handle strong discontinuities. We show by comparing the solutions with the exact one that mesh convergence to the proper weak solution is indeed reached.

2. GENERAL PRINCIPLE, FIRST-ORDER VERSION OF THE SCHEME

We start from the first-order upwind scheme

$$W_i^{n+1} = W_i^n - \lambda[F_{i+1/2} - F_{i-1/2}].$$

In what follows, the formulation (5) is used, but any other formulation might have been employed here. In this paragraph, we first examine the behavior of a contact discontinuity with Roe's scheme. Latter on, we discuss what happens with other schemes. For the sake of simplicity, we assume that the pressure and the velocity are uniform throughout the computational grid. What we have in mind is to find a condition that enable this contact discontinuity to remain a contact discontinuity, i.e., $u_i^{n+1} = u_i^n \equiv u$ and $p_i^{n+1} = p_i^n \equiv p$ for any indices i.

The numerical flux $F_{i+1/2} = F(W_i, W_{i+1})$ is given by Roe's linearization,

$$F(W_L, W_R) = \tfrac{1}{2}[F(W_L) + F(W_R) - |\overline{A}|(W_R - W_L)].$$

The matrix $\overline{A}$ depends on $\overline{Y^{(1)}}, \overline{Y^{(2)}}, \overline{u}, \overline{H}, \overline{\chi_j} = \overline{\partial p}/\partial \rho_j$ ($j = 1, 2$) and $\overline{\kappa} = \overline{\partial p}/\partial \varepsilon$. They have the following values:

$$\overline{Y^{(j)}} = \frac{\sqrt{\rho_L}Y_L^{(j)} + \sqrt{\rho_L}Y_R^{(j)}}{\sqrt{\rho_L} + \sqrt{\rho_R}}, \quad j = 1, 2,$$
$$\overline{u} = \frac{\sqrt{\rho_L}u_L + \sqrt{\rho_R}u_R}{\sqrt{\rho_L} + \sqrt{\rho_R}}$$
$$\overline{H} = \frac{\sqrt{\rho_L}H_L + \sqrt{\rho_R}H_R}{\sqrt{\rho_L} + \sqrt{\rho_R}}.$$

The value of $\overline{\kappa}$ is given by (4), where $Y^{(1)}$ and $Y^{(2)}$ are replaced by the corresponding average values defined above. Those of $\overline{\chi_i}$ are replaced in such a way that

$$\Delta p = \overline{\chi_1}\Delta\rho^{(1)} + \overline{\chi_2}\Delta\rho^{(2)} + \overline{\kappa}\Delta\varepsilon, \tag{8}$$

we have set $\Delta\rho^{(j)} = \rho_L^{(j)} - \rho_R^{(j)}$, etc. to simplify the notations; see [1], for example.

Assume now that the three states $W_{i+1}^n, W_i^n, W_{i-1}^n$ have the same pressure p and the same velocity u. A straightforward calculation shows that if one sets

$$\Delta_{i+1/2} = \rho_{i+1} - \rho_i, \qquad \Delta'_{i+1/2} = \frac{1}{\kappa_{i+1}^n} - \frac{1}{\kappa_i^n},$$
$$\Delta_{i+1/2}^{(1)} = \rho_{i+1}^{(1)} - \rho_i^{(1)}, \quad \Delta_{i+1/2}^{(2)} = \rho_{i+1}^{(2)} - \rho_i^{(2)},$$

we get

$$|\overline{A_{i+1/2}}|(W_{i+1}^n - W_i^n) = \begin{pmatrix} |u|\Delta_{i+1/2}^{(1)} \\ |u|\Delta_{i+1/2}^{(2)} \\ |u|u\Delta_{i+1/2} \\ |u|\dfrac{u^2}{2}\Delta_{1/2} + p\Delta'_{1/2} \end{pmatrix}.$$

Here we have taken into account the relation (8) with $\Delta p = 0$.

Using all this, it is easy to see that

$$\begin{aligned} \rho_i^{n+1} &= \rho_i^n - \lambda(u(\Delta_{1/2} + \Delta_{-1/2}) - |u|(\Delta_{1/2} - \Delta_{-1/2})) \\ u_i^{n+1} &= u \\ E_i^{n+1} &= E_i^n - \lambda\left(\frac{up}{2}[\Delta'_{1/2} + \Delta'_{-1/2}] - \frac{|u|u}{2}[\Delta'_{1/2} - \Delta'_{-1/2}]\right. \\ &\quad \left. + \frac{u^2}{4}[\Delta_{1/2} + \Delta_{-1/2}] - \frac{|u|u^2}{4}[\Delta'_{1/2} - \Delta'_{-1/2}]\right). \end{aligned} \tag{9}$$

Since $E_i^n = p/\kappa_i^n + \frac{1}{2}\rho_i^n u^2$ and $E_i^{n+1} = p_i^{n+1}/\kappa_i^{n+1} + \frac{1}{2}\rho_i^{n+1}u^2$, we can see that a necessary condition for $p_i^{n+1} = p$ is

$$\frac{1}{\kappa_i^{n+1}} = \frac{1}{\kappa_i^n} - \frac{\lambda}{2}(u_i^n[\Delta'_{1/2} + \Delta'_{-1/2}] - |u_i^n|[\Delta'_{1/2} - \Delta'_{-1/2}]). \tag{10}$$

Equation (10) is nothing more than a discretization of

$$\left(\frac{1}{\kappa}\right)_t + u\left(\frac{1}{\kappa}\right)_x = 0.$$

All together, our numerical scheme is the following:

1. the update of ρ, ρu, and E by the classical multispecies Roe scheme,
2. the update of $1/\kappa_i^n$ by (10). The mass fractions $Y^{(1),n+1}$ and $Y^{(2)n+1}$ are obtained by inverting (4).

Since $1/\kappa_i^n \in [\min_i(1/\kappa_i^0), \max_i(1/\kappa_i^0)]$ if $\lambda \max_i |u_i^n| \leq 1$, the mass fractions $Y^{(1)}$ and $Y^{(2)}$ remain in $[0, 1]$ with the same CFL condition as in the original scheme.

3. HIGH ORDER EXTENSIONS

We assume that a high order extension of the original finite volume scheme is obtained through the MUSCL method. In each cell, we get a reconstruction of the conservative variables:

$$W_i^n(x) = W_i^n + \delta W^n(x). \tag{11}$$

The slope is computed so that the average of (11) in $[x_{i-1/2}, x_{i+1/2}]$ is W_i^n. The variation $\delta W(x)$ is obtained by computing slopes either on the primitive or characteristic variables.The slope may be limited with the help of limiters, or computed with the help of the ENO method. In both cases, we assume that if all the points of the stencil used to compute δW share the same pressure p and the same velocity u, then the velocity and the pressure defined by (11) are u and p.

To simplify the text, we assume that the standard high order finite volume scheme is the following second-order scheme:

$$W_i^{n+1/2} = W_i^n - \frac{\lambda}{2}(F(W_i^{n+}) - F(W_i^{n-})) \tag{12a}$$
$$W_i^{n+1} = W_i^n - \lambda(F(W_i^{n+1/2+}, W_{i+1}^{n+1/2-}) - F(W_{i-1}^{n+1/2+}, W_i^{n+1/2-})) \tag{12b}$$

Here, we have set for $l = n$ or $n + 1/2$,

$$W_i^{l+} = W_i^l + \delta W^l\left(\frac{\Delta x}{2}\right),$$

$$W_i^{l-} = W_i^l + \delta W^l\left(\frac{-\Delta x}{2}\right).$$

The exact flux is used in the predictor step, while the Roe flux is employed in the corrector one.

To construct our multicomponent scheme, the simplest way is to update $1/\kappa$ in such a way that an initial condition made of a contact discontinuity (with velocity u and pressure p) will remain a contact discontinuity. In order to simplify the text, we introduce, for any $w = p$, u or p the following notations:

$$w_{i+1/2}^{\pm} = \begin{cases} w_i + \tfrac{1}{2}\delta w_i, \\ w_{i+1} - \tfrac{1}{2}\delta w_{i+1}. \end{cases}$$

The δw_i are computed from (11). Their expressions depend on the kind of variable we have used to define δW. The slope limitation should be done in such a way that if the pressure and the velocity are uniform, then the extrapolated pressure and velocity should also be uniform.

According to the assumptions we have made, if at time t_n, W^n defines a contact discontinuity, and we have

$$\rho_{i+1/2}^{+} = \rho_i^n + \tfrac{1}{2}\delta\rho_i, \qquad \rho_{i+1/2}^{-} = \rho_{i+1}^n - \tfrac{1}{2}\delta\rho_{i+1}$$

$$u_{i+1/2}^{\pm} = u_i^n = u_{i+1}^n, \qquad p_{i+1/2}^{\pm} = p_i^n = p_{i+1}^n$$

$$\frac{1}{\kappa_{i+1/2}^{+}} = \frac{1}{\kappa_i^n} + \frac{1}{2}\delta\left(\frac{1}{\kappa_i}\right), \quad \frac{1}{\kappa_{i+1/2}^{-}} = \frac{1}{\kappa_{i+1}^n} - \frac{1}{2}\delta\left(\frac{1}{\kappa_{i+1}}\right).$$

Some straightforward calculations show that after the predictor step, the velocity remains the same and the pressure also remains invariant, provided that

$$\frac{1}{\kappa_i^{n+1/2}} = \frac{1}{\kappa_i^n} - \lambda u_i^n\left(\frac{1}{\kappa_{i+1/2}^{+}} - \frac{1}{\kappa_{i+1/2}^{-}}\right). \tag{13}$$

Then, the same result is true after the corrector step, provided that $1/\kappa$ is updated by

$$\begin{aligned} \frac{1}{\kappa_i^{n+1}} &= \frac{1}{\kappa_i^n} - \frac{\lambda}{2}\left(u_i^{n+1/2}[\Delta'_{1/2} - \Delta'_{-1/2} + \delta^+]\right. \\ &\quad \left. - |u_i^{n+1/2}|[\Delta'_{1/2} - \Delta'_{-1/2} - \delta^-]\right) \\ \delta^+ &= \tfrac{1}{2}(\delta_{i+1}^{n+1/2} - 2\delta_i^{n+1/2} + \delta_{i-1}^{n+1/2}) \\ \delta^- &= \tfrac{1}{2}(\delta_{i+1}^{n+1/2} - \delta_{i-1}^{n+1/2}). \end{aligned} \tag{14}$$

In Eqs. (14), δ_l^p stands for $\delta(1/\kappa_l^p)$.

Our modified scheme is the following:

TABLE I

Initial Conditions

State	Y	ρ	u	p (in Pa)
Left (helium)	1.	14.54903	0.	194.3×10^5
Right (air)	0	1.16355	0	10^5

1. Predictor step. Update ρ, ρu, and E by (12a) and $1/\kappa$ by (13),
2. Corrector step. Update ρ, ρu, and E by (12b) and $1/\kappa$ by (14).

All our numerical experiments show that this scheme is stable under the same CFL condition. The mass fractions remain positive. An analysis is provided in the Appendix.

4. NUMERICAL EXPERIMENTS

In this section, we want to illustrate this methodology, to compare it to the existing finite volume one, and to show it can handle strong shocks. We also wish to check whether the numerical solution converges to the weak one.

4.1. *Comparison with Finite Volume Schemes*

We consider the test case defined in Table I. The ratio of specific heats are respectively 1.67 and 1.4. The specific heats are respectively $c_v = 2420$ and $c_v = 732$ (International Unit System). Figures 1, 2, 3, 4 give the density, velocity, pressure, and $\gamma - 1$ for the first-order scheme. This example is interesting because it indicates a very vicious behavior of fully conservative finite volume schemes for multicomponent flows. The mesh has 101 cells. From Figs. 1, 2, 4 one can see that both schemes behave the same. The only visible difference lies in Fig. 4 (where the conservative scheme seems even less dissipative) and mainly in the density, Fig. 3, where the classical scheme exhibits a small undershoot. The contact discontinuity is also extremely smeared. In order to improve the results, we now apply the MUSCL technique on the characteristic variables. While the results on the velocity and the pressure (Figs. 5, 6, 7, 8) are still of the same quality, with the same remark for κ, the density shows a very different behavior; there is a very large undershoot for the classical scheme, which is not true for the one we propose.

We also present some computational results on Karni and Quirk's test case (Table II). It consists of a shock tube filled with air ($\gamma = 1.4$, $c_v = 0.72$), where a shock wave moves to the right. In the preshock wave state, a bubble of helium is set ($\gamma = 1.67$, $c_v = 2.42$) (C.G.S. unit system). We use 201 cells, the shock wave is initially at $x = 0.25$, and the bubble sits between $x = 0.4$ and $x = 0.6$. The

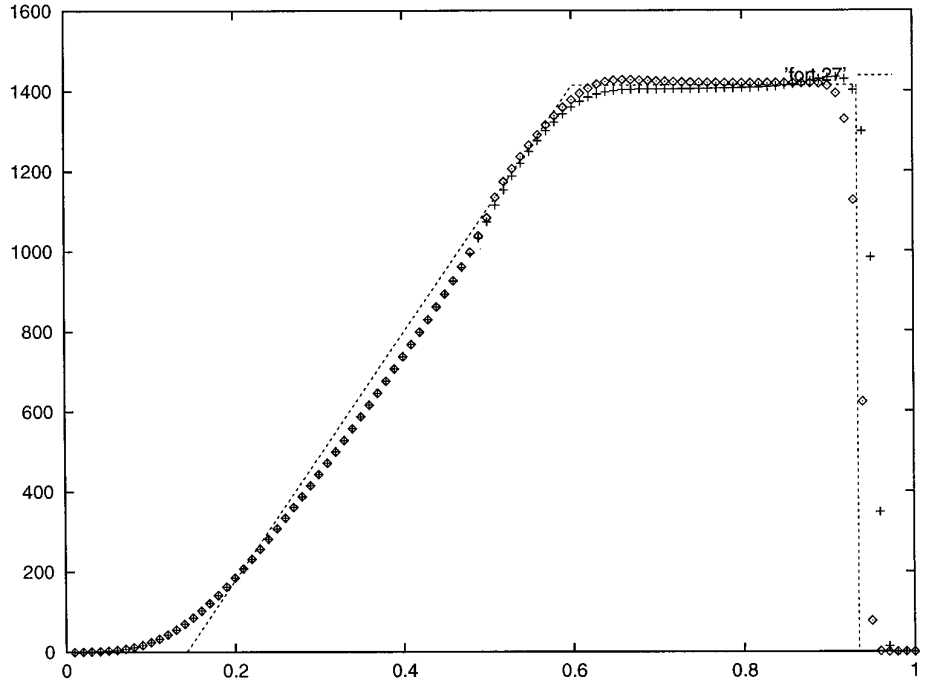

FIG. 1. Velocity, 1st order: ◇, present scheme; +, finite volume scheme of [5]; dotted line, exact solution.

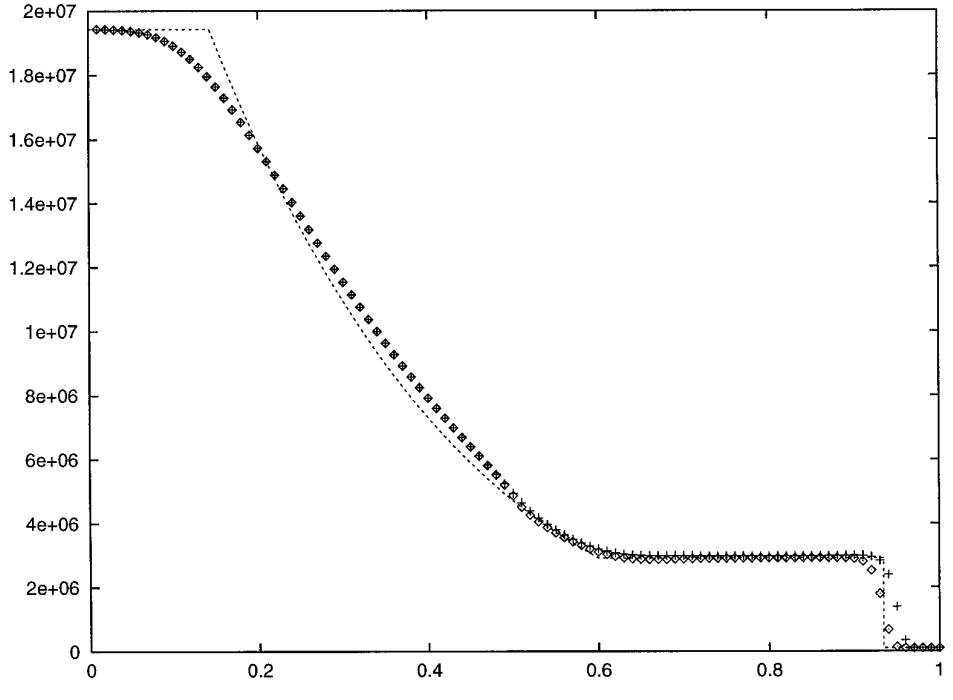

FIG. 2. Pressure, 1st order: ◇, present scheme; +, finite volume scheme of [5]; dotted line, exact solution.

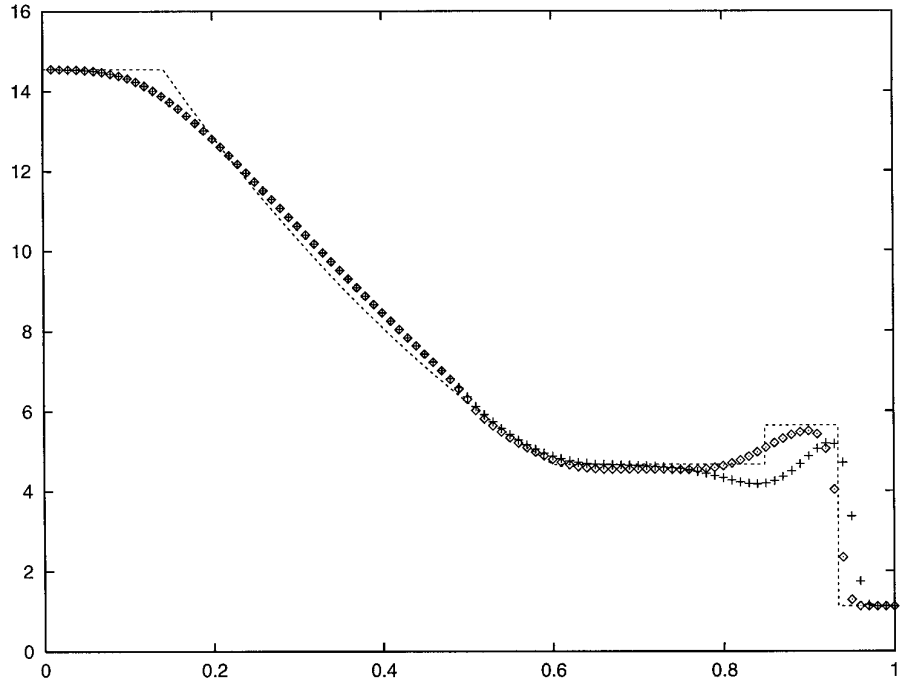

FIG. 3. Density, 1st order: ◇, present scheme; +, finite volume scheme of [5]; dotted line, exact solution.

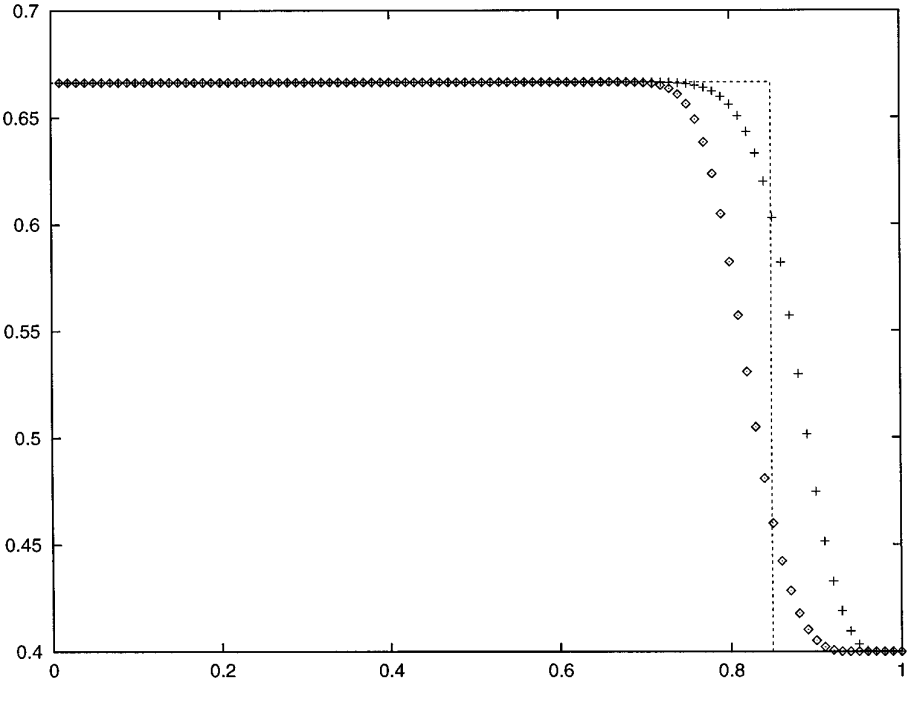

FIG. 4. $\gamma - 1$, 1st order: ◇, present scheme; +, finite volume scheme of [5]; dotted line, exact solution.

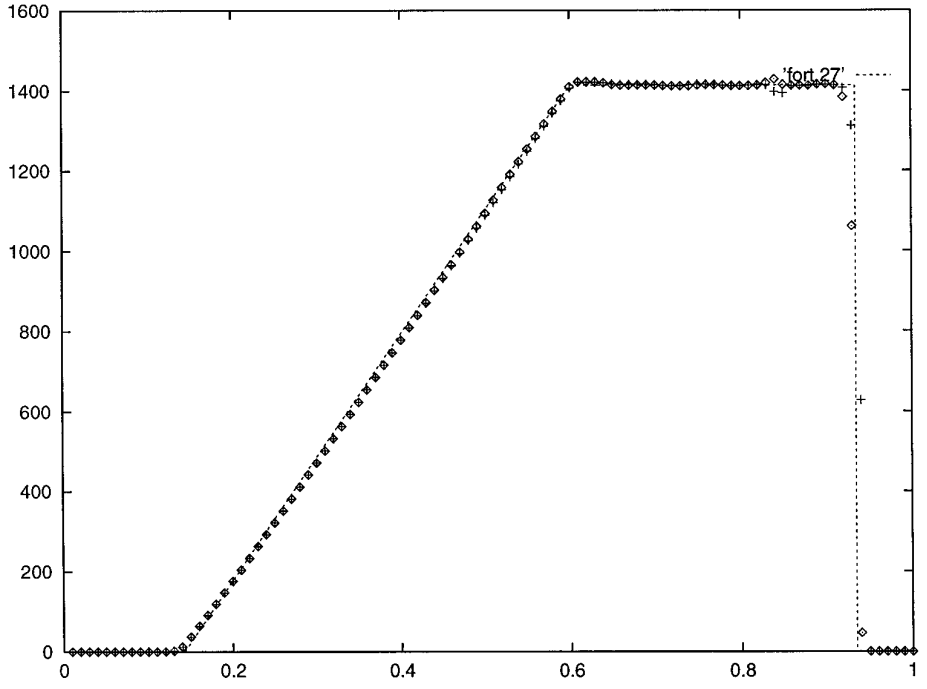

FIG. 5. Velocity, 2nd order: ◇, present scheme; +, finite volume scheme of [5]; dotted line, exact solution.

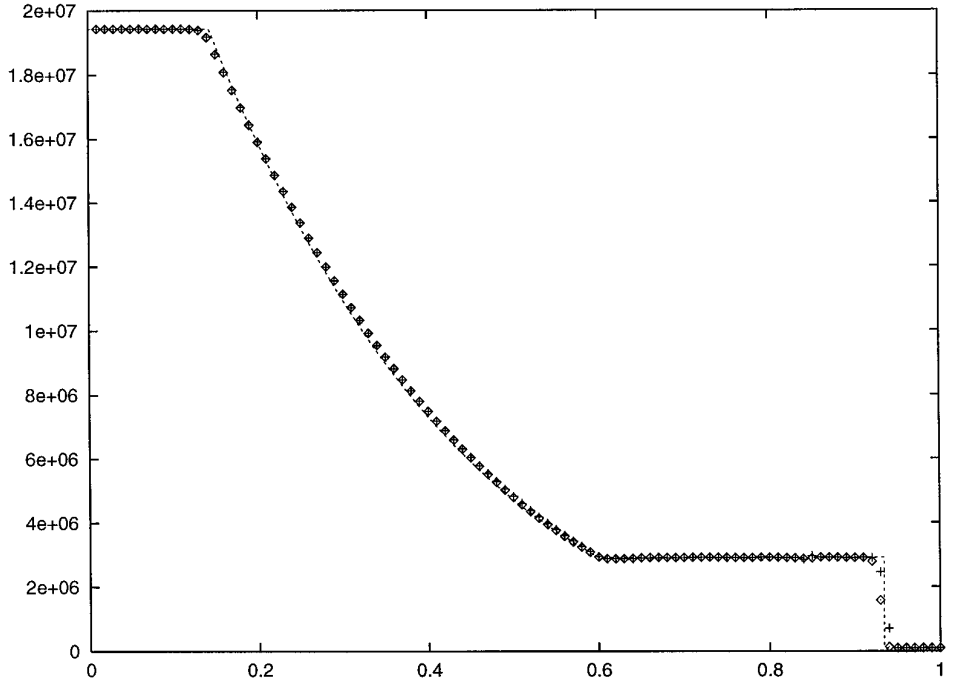

FIG. 6. Pressure, 2nd order: ◇, present scheme; +, finite volume scheme of [5]; dotted line, exact solution.

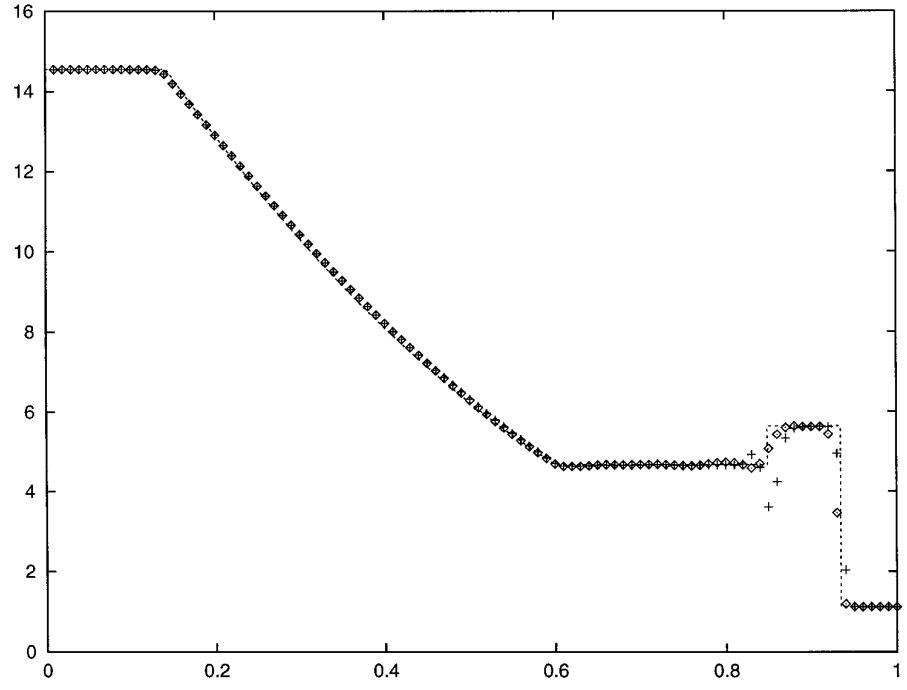

FIG. 7. Density, 2nd order: ◇, present scheme; +, finite volume scheme of [5]; dotted line, exact solution.

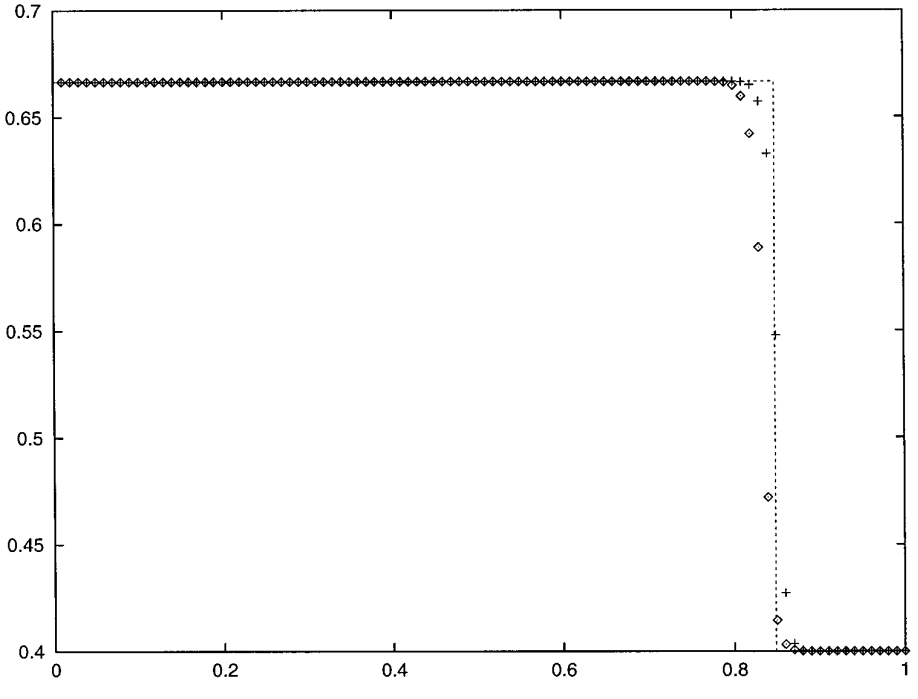

FIG. 8. $\gamma - 1$, 2nd order: ◇, present scheme; +, finite volume scheme of [5]; dotted line, exact solution.

TABLE II

Shock/Bubble Interaction

	Y_1	ρ	u	p
Postshock	1	1.3765	0.3948	1.57
Preshock	1	1	0	1
Bubble	0	0.138	0	1

TABLE III

Initial Conditions for the Convergence Study

	Y_1	ρ	$-u$	p	γ
Left	1	1	0	10	1.6
Right	0	2	−1	0.1	1.4

results are presented at time $t = 0.35$, are obtained with the second-order version of both schemes with extrapolation on the characteristic variable. The CFL number is 0.75. Figure 9a shows the pressure obtained with the present scheme, while Fig. 9b shows what is obtained with the conservative scheme of [5]. Spurious oscillations, as with Quirk and Karni's results are visible for the conservative scheme and are absent for the present scheme.

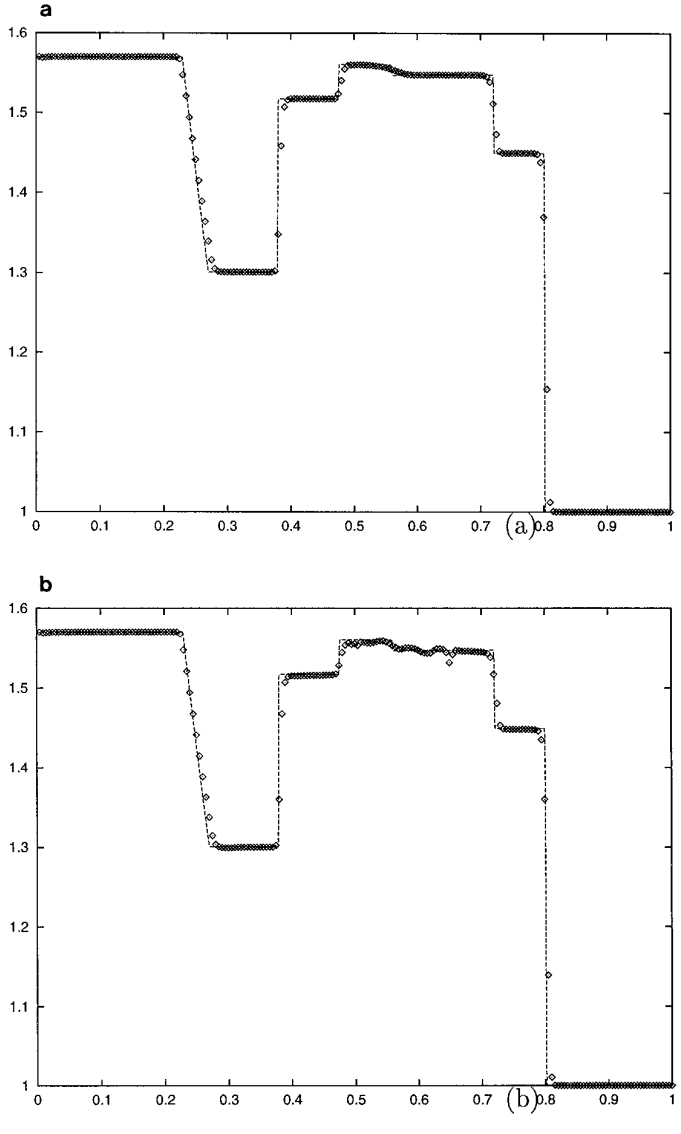

FIG. 9. Pressure, 2nd order: present scheme (a); conservative scheme (b); dotted lines, exact solution.

We can see with these figures, that our new scheme also behaves much better than the old one; no oscillations at all are visible. This conclusion is the same for each test case we have run.

5. CONVERGENCE TO THE CORRECT WEAK SOLUTION

This point is studied numerically. The new scheme is tested with 5001 mesh points in its second-order version (reconstruction on the primitive variables). A new test case is employed, to get stronger discontinuities (Table III). The shock Mach number (defined as $(U_{\text{shock}} - u_R)/a_R$ is 7.97; its velocity is 1.11. The contact discontinuity velocity is 0.73; its pressure is 7.40. We present the density in [0, 1] (Fig. 10) and a zoom (Fig. 11) that enable us to better see the contact discontinuity and the shock wave. We clearly see that the numerical solution is very close to the exact one. In particular, the correct levels of density are obtained and the discontinuities move at the right speed. The first conclusion is true, whatever the variable (pressure, velocity, κ, or Mach number).

This conclusion is not really surprising; γ does not change in a fan or a shock wave and the present scheme is nothing more than the classical one in this case. In a contact discontinuity, the gradient of the velocity must vanish. Since we integrate simultaneously the approximations of

$$\rho_t + (\rho u)_x = 0, \quad \left(\frac{1}{\kappa}\right)_t + u\left(\frac{1}{\kappa}\right)_x = 0,$$

it is legitimate to expect the right contact discontinuity speed.

6. CONCLUSION

We have presented a new scheme for multispecies compressible flow simulations. It is constructed to suppress or minimize the spurious oscillations that are generated by conventional finite volume schemes. This property is also

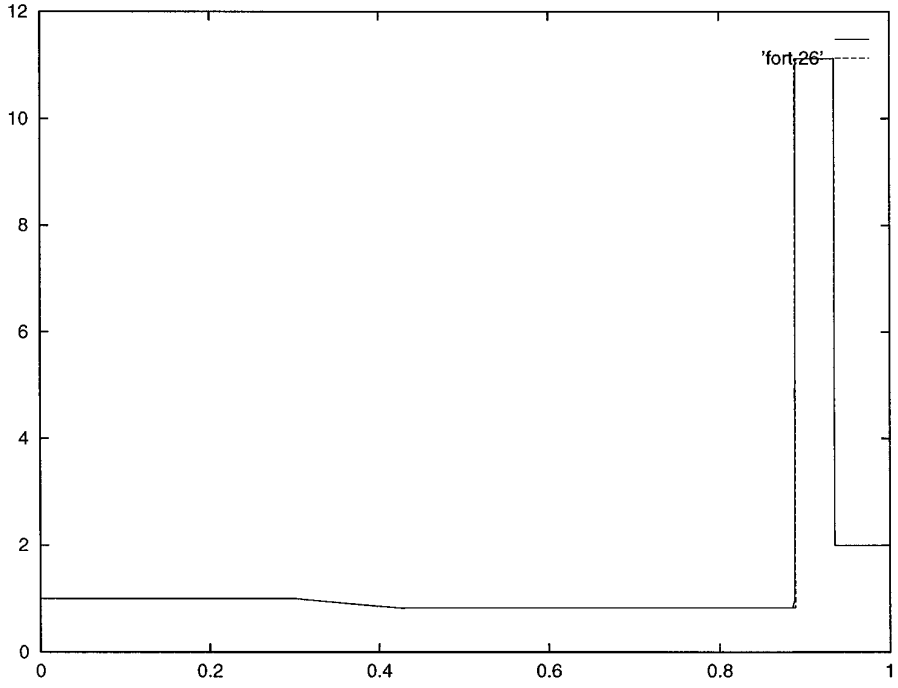

FIG. 10. Density, 2nd order, 5001 mesh points: ◇, present scheme; dotted line, exact solution.

true for Karni's scheme, but the present one, from its construction, is able to handle strong shocks. Nevertheless, note the recent developments of [10].

The present analysis has been done with the help of a Roe scheme. The same construction could have been done for any finite volume constructed from a Riemann solver; the key property which is needed is that, in an exact contact discontinuity, after one time step the velocity should remain uniform. This is not true for the van Leer scheme; thus the present construction cannot be extended. One remedy would be to apply the hybridation technique of Coquel and Liou [9].

The extension to more that one dimension has not yet been carried out. We wish to do it in the near future. This extension should be done according to the same principles. Nevertheless, one should notice that in more than one dimension, pressure oscillation may be created, even for a single species gas, when the slip lines are aligned with the mesh; this new phenomenon should be included in the analysis.

Extensions to more that two species is straightforward (consider $W = (\rho, \rho_1, ..., \rho_{ns-2}, 1/\kappa, \rho u, E)$ and apply the same principles).

APPENDIX A: ANALYSIS OF THE SECOND-ORDER SCHEME

We assume that the scheme on the density, momentum, and total energy is stable under a given CFL condition. We are interested in the behavior of $1/\kappa$. We assume that $1/\kappa_i^0 \in [a, b]$. We recall that the predictor–corrector scheme is given by:

1. at each time step, staring from the values $(\rho_i^n, \rho_i^n u_i^n, E_i^n, 1/\kappa_i^n)^{\mathrm{T}}$, one evaluates slopes on the physical variables $(\rho, u, p, 1/\kappa)$ or the characteristic variables $(\alpha_u, \alpha_{u+c}, \alpha_{u-c}, 1/\kappa)$.

2. Slope limiters are used in order to avoid the creation of new extremas. In particular, the limitation on $1/\kappa$ is done in such a way that the reconstructed values $1/\kappa_{i\pm1/2}^n$ at the cells interfaces $x_{i\pm1/2}$ satisfy

$$\min_{|i-j|\le 1} \frac{1}{\kappa_j^n} \le \frac{1}{\kappa_{i\pm1/2}^n} \le \max_{|i-j|\le 1} \frac{1}{\kappa_j^n}.$$

This is satisfied by the minmod limiter.

3. The scheme (12a) and (13) is applied.

4. We then reuse the same limited slopes to evaluate the values $W_{i\pm1}^{n+1/2}$ in the scheme (12a, 14)

To simplify the notations, we set

$$u^+ = \tfrac{1}{2}(u_i^{n+1/2} + |u_i^{n+1/2}|), \quad u^- = \tfrac{1}{2}(u_i^{n+1/2} - |u_i^{n+1/2}|;$$

these are the positive and negative parts of $u_i^{n+1/2}$.

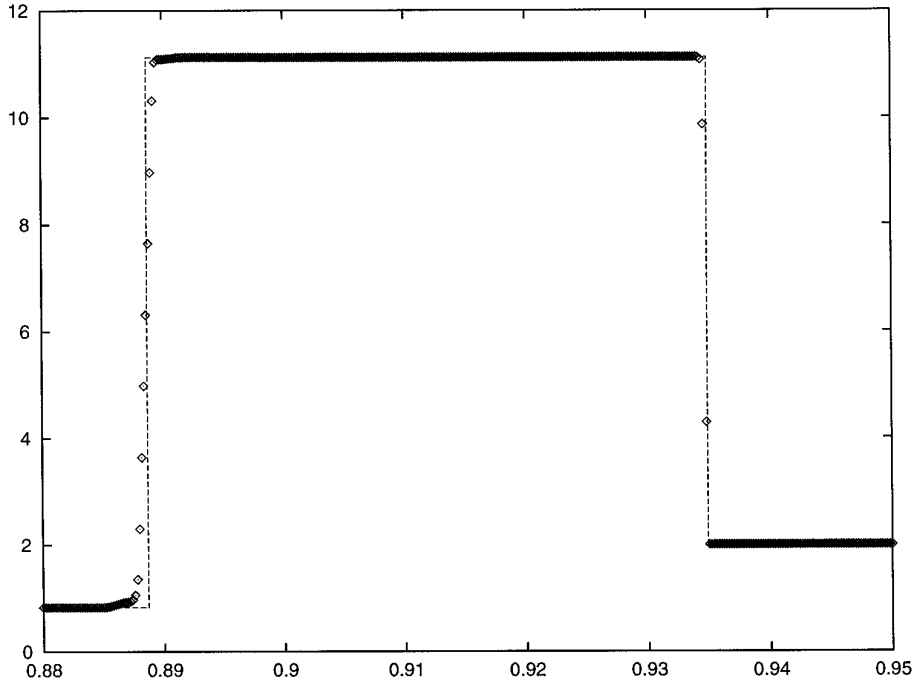

FIG. 11. Zoom of the density, 2nd order, 5001 mesh points: ◇, present scheme; dotted line, exact solution.

Since $1/\kappa_i = \frac{1}{2}(1/\kappa^-_{i+1/2} + 1/\kappa^+_{i-1/2})$, one can rewrite (14) as

$$\frac{1}{\kappa_i^{n+1}} = \left(\frac{1}{2} - \lambda u^+\right)\frac{1}{\kappa^-_{i+1/2}} + \lambda u^+ \frac{1}{\kappa^-_{i-1/2}} + \left(\frac{1}{2} + \lambda u^-\right)\frac{1}{\kappa^+_{i-1/2}} - \lambda u^- \frac{1}{\kappa^+_{i+1/2}}.$$

From the definition of u^+ and u^-, the coefficients in front of the $(1/\kappa)$'s are positive, provided that $\lambda|u_i^{n+1/2}| \leq \frac{1}{2}$. We conclude that $1/\kappa_i^{n+1} \in [a, b]$, thanks to the properties of the slope limitation.

In practice, $1/\kappa$ is limited by the minmod limiter. It is the one that gives the best results, especially in example 1. The slopes have been recomputed at each half time step, but the difference when an evaluation is made at each time step is very small. Last, the CFL condition $\lambda|u_i^{n+1/2}| \leq \frac{1}{2}$ is relaxed to $\lambda|u_i^{n+1/2}| \leq 1$.

ACKNOWLEDGMENTS

I thank S. Karni and J. J. Quirk for their support in this study. M. Cardoso (University of Provence, France) provided me with the first numerical example.

REFERENCES

1. R. Abgrall, *Rech. Aerosp.* **6** (1988).
2. D. Chargy, R. Abgrall, L. Fezoui, and B. Larrouturou, *Rech. Aerosp.* **2** (1992).
3. T. Y. Hou and P. Le Floch, *Math. Comput.* **62**(206) (1994).
4. S. Karni, *SIAM J. Numer. Anal.* **29** (1992).
5. S. Karni, *J. Comput. Phys.* **112** (1994).
6. B. Larrouturou, *J. Comput. Phys.* **95** (1991).
7. J. J. Quirk and S. Karni, Technical Report 94-75, ICASE, 1994 (unpublished).
8. P. L. Roe. Technical report, Cranfield Institute of Technology, 1984 (unpublished).
9. F. Coquel and M.-S. Liou, "Stable and Low Diffusive Upwind Splitting Methods, in *Computational Fluid Dynamics* '92, Vol. 1, edited by Périaux and Hirsch (Elsevier Science, New York, 1992), p. 9.
10. S. Karni, Courant Mathematics and Computing Lab report No. 95-001, 1995 (unpublished).